

Structure-Guided Design of Cell Wall Biosynthesis Inhibitors That Overcome β -Lactam Resistance in *Staphylococcus aureus* (MRSA)

Carlos Contreras-Martel,^{†,‡,§,¶} Ana Amoroso,^{¶,¶} Esther C. Y. Woon,^{†,¶} Astrid Zervosen,^{#,¶} Steven Inglis,[†] Alexandre Martins,^{†,‡,§} Olivier Verlaine,[¶] Anna M. Rydzik,[†] Viviana Job,^{†,‡,§} André Luxen,[#] Bernard Joris,[¶] Christopher J. Schofield,^{†,*} and Andréa Dessen^{†,‡,§,*}

[†]Bacterial Pathogenesis Group, Institut de Biologie Structurale, Université Grenoble I, [‡]Commissariat à l'Énergie Atomique (CEA), and [§]Centre National pour la Recherche Scientifique (CNRS), 41 rue Jules Horowitz, 38027 Grenoble, France

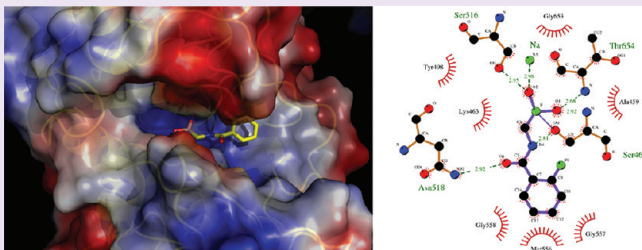
[¶]Centre d'Ingénierie des Protéines, Institut de Chimie, B6a, Université de Liège, Sart Tilman, B4000 Liège, Belgium

[†]Chemistry Research Laboratory, University of Oxford, 12 Mansfield Road, Oxford OX1 3TA, U.K.

[#]Centre de Recherches du Cyclotron, B30, Université de Liège, Sart Tilman, B4000 Liège, Belgium

S Supporting Information

ABSTRACT: β -Lactam antibiotics have long been a treatment of choice for bacterial infections since they bind irreversibly to Penicillin-Binding Proteins (PBPs), enzymes that are vital for cell wall biosynthesis. Many pathogens express drug-insensitive PBPs rendering β -lactams ineffective, revealing a need for new types of PBP inhibitors active against resistant strains. We have identified alkyl boronic acids that are active against pathogens including methicillin-resistant *S. aureus* (MRSA). The crystal structures of PBP1b complexed to 11 different alkyl boronates demonstrate that *in vivo* efficacy correlates with the mode of inhibitor side chain binding. Staphylococcal membrane analyses reveal that the most potent alkyl boronate targets PBP1, an autolysis system regulator, and PBP2a, a low β -lactam affinity enzyme. This work demonstrates the potential of boronate-based PBP inhibitors for circumventing β -lactam resistance and opens avenues for the development of novel antibiotics that target Gram-positive pathogens.



The spread of antibiotic resistance by bacterial pathogens, coupled to a decrease in the rate of discovery of novel antibiotics, has had a devastating effect on the potential for treatment of many infections by small molecules. Methicillin-resistant *Staphylococcus aureus* (MRSA) causes both hospital- and community-acquired infections that lead to a high mortality rate, and the likelihood that MRSA will develop resistance to the “last resort” antibiotic vancomycin is a matter of concern. *Streptococcus pneumoniae* and *Enterococcus faecium* strains insensitive to β -lactam antibiotics are being increasingly identified in hospitals worldwide.¹ In addition, the few novel families of antimicrobials, e.g., linezolid, have already elicited the appearance of resistance in different pathogens,² underlining the continuing need for the development of pharmaceuticals that are effective against drug-resistant organisms.

Stability of the peptidoglycan (PG), an essential component of the bacterial cell wall, is a requirement both for cell viability and growth, and targeting of its biosynthesis machinery can lead to bacterial lysis and death. The PG is composed of alternating GlcNAc and MurNAc units cross-linked by short peptides.³ Penicillin-Binding Proteins (PBPs) catalyze the transpeptidation (TP) and carboxypeptidation (CP) reactions that cross-link stem peptides and regulate PG cross-linking, respectively.^{4–7}

The PBP TP/CP reaction mechanisms involve the formation of acyl–enzyme complexes by reaction of the C-terminal D-Ala-D-Ala group of the PG stem peptide with a nucleophilic serine of the PBP. The same serine is acylated by β -lactam antibiotics to generate a stable acyl–enzyme complex that is at the basis of the efficacy of β -lactams as antibacterial agents.

The catalytic sites of PBPs reside on the exterior of the bacterial cell wall, allowing ligand access without the need to cross the lipid bilayer. Thus, PBPs remain excellent targets for antibacterial development. However, pathogens such as *S. pneumoniae* produce β -lactam-resistant PBPs that are recalcitrant toward β -lactam recognition due to the presence of mutations, notably in the active site region; *E. faecium* and *S. aureus* also produce antibiotic-insensitive PBPs.^{8–11} The two latter pathogens also secrete β -lactamases that catalyze the hydrolysis of β -lactams, generating inactive β -amino acids. These observations reveal the need for the development of non- β -lactam antibiotics for treatment of β -lactam-resistant infections.¹² The feasibility of this strategy has been shown for γ -lactams, which kill

Received: February 22, 2011

Accepted: July 6, 2011

Published: July 06, 2011

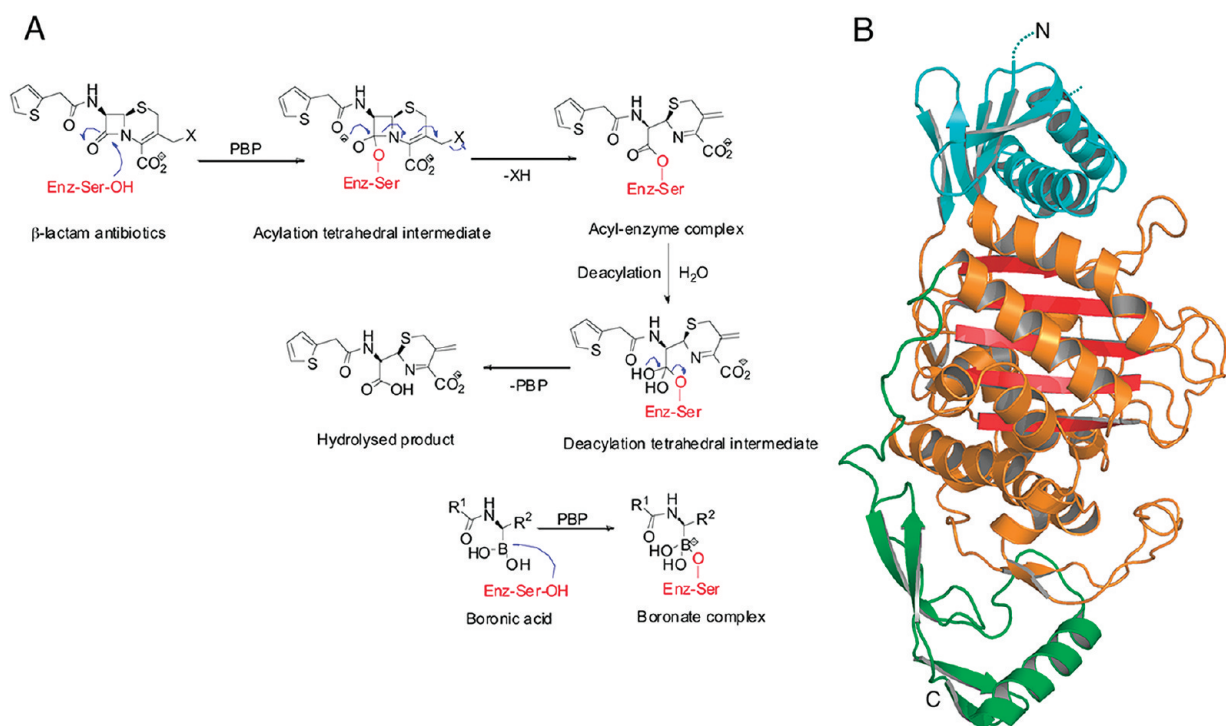


Figure 1. The transpeptidase domain of PBPs is the target of β -lactams and boronates. (A) Reaction of PBPs with boronic acid inhibitors and β -lactam antibiotics. (B) The overall structure of PBP1b displays a truncated GT domain (N-terminal), a linker region, and a C-terminal TP domain.²⁷

β -lactam-resistant bacteria.^{13–15} However, like β -lactams, γ -lactams are irreversibly acylating agents and are thus also likely to be susceptible to the development of β -lactamase-mediated resistance. To date, there are very few reports of reversibly binding non-lactam PBP inhibitors, and no such compounds are used clinically.

Functionalized boronic acids inhibit nucleophilic enzymes, including β -lactamases, *via* the reversible formation of a covalent complex proposed to mimic the tetrahedral catalytic intermediate (Figure 1a¹⁶). Both small molecule and peptide boronic acid based inhibitors of these enzymes have been described,^{16–26} but none have been reported to possess any significant antibacterial activity. By employing PBP1b from the pathogen *S. pneumoniae* as a model enzyme, we have pursued a crystallography-guided approach to identify effective PBP1b inhibitors for analysis as antibacterials. High-resolution crystal structures of PBP1b covalently associated to 11 boronic acid analogues reveal distinct side chain binding modes and rationalize the different inhibitory potencies observed for the various ligands. Importantly, we identify boronic acid inhibitors that display antibacterial activity against clinically relevant pathogens including methicillin-resistant *Staphylococcus aureus* (MRSA) by targeting essential PBPs *in vivo*. These results imply that the molecules identified in this work will be useful for the development of non- β -lactam antibiotics against drug-resistant bacteria.

RESULTS AND DISCUSSION

Inhibition of a PG-Biosynthesis Enzyme by Boronate Transition State Analogues. We began by employing a structure-based fragment screen by soaking boronic acids substituted with small groups into crystals of PBP1b.²⁷ Although the major antibiotic resistance determinant in *S. pneumoniae* is PBP2x,²⁸

PBP1b was employed in this study because PBP1b crystals that diffract X-rays to high resolution can be prepared quickly and reproducibly, thus making it an optimal model enzyme. PBP1b is an elongated protein that can be described as possessing “head”, “neck”, and “body” regions, which correspond approximately to a short N-terminal peptide from the GT domain, the GT/TP linker region, and the C-terminal TP domain (Figure 1b); in the structures reported here, the GT domain of PBP1b is truncated, following a trypsinolysis step during the purification protocol that was required for the preparation of well-diffracting crystals.²⁷

Previously, we had determined that the active site of wild type PBP1b is naturally in a “closed” conformation due to a hydrogen bond contributed by Asn656. Thus, in order to obtain crystal structures of this form of PBP1b in the presence of small molecules, it was necessary to perform time-consuming preincubation steps in the presence of a pseudosubstrate prior to ligand soaking steps.^{27,29} In order to circumvent this problem, we generated a PBP1b Asn656Gly mutant in which the active site remains in an “open” conformation. The structure was solved by molecular replacement using the native PBP1b structure as a model.²⁷ This strategy allowed us to obtain an initial 2.1 Å crystal structure of PBP1b with S6 (Supplementary Table S1), a phenyl boronic acid.

The PBP1b active site is formed by three conserved catalytic motifs: Ser-X-X-Lys, which harbors the nucleophilic Ser460, Ser516-X-Asn518, and Lys651-Thr-Gly (Figure 2a). In the complex between PBP1b and S6, electron density corresponding to the boronic acid inhibitor clearly indicates that O γ of Ser460 makes a covalent bond with the boron atom and forms a tetrahedral complex. The acetamido side chain of S6 is positioned similarly to that of PBP β -lactam acyl-enzyme complexes;²⁷ however, the active site region remains largely unoccupied due to the small size of the S6 side chain

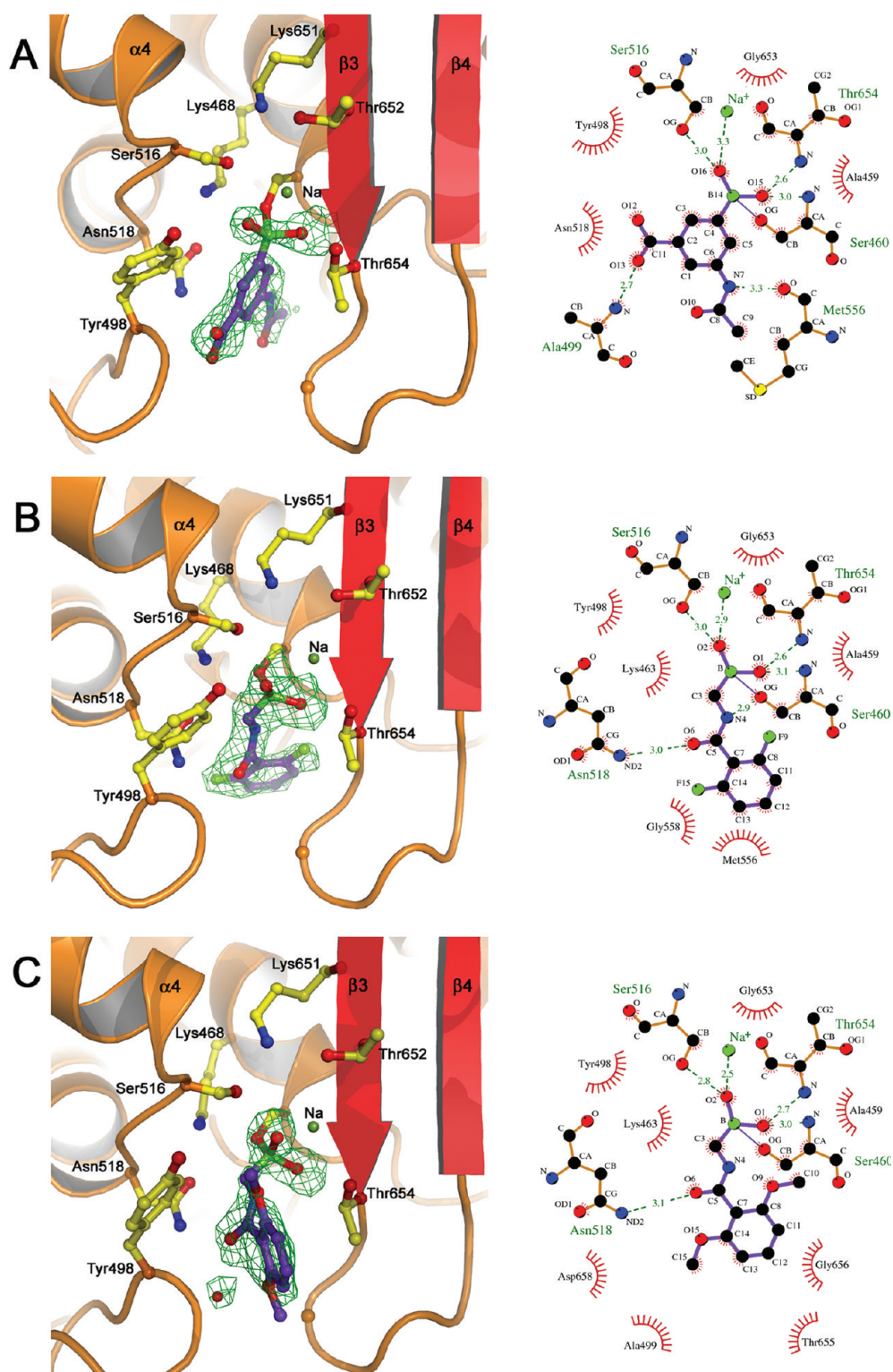
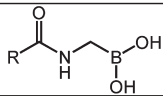
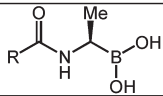
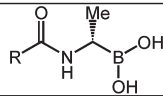
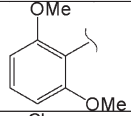
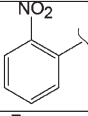
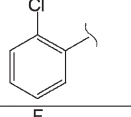
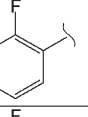
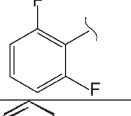
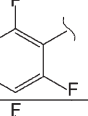
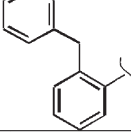
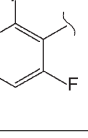
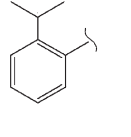
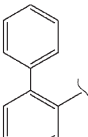


Figure 2. Details of the active sites of structures of PBP1b complexed to (A) S6, (B) AS, and (C) A1. Left, $F_o - F_c$ maps contoured to 3.0σ calculated prior to inclusion of the ligands in refinement protocols are shown in green. Side chains are shown as ball-and-stick, with carbon atoms corresponding to the ligand in purple and those corresponding to the protein in yellow. (right) Ligplot analyses of the neighborhood of the ligands within the cleft.

(Figure 2a), implying weak binding, and is consistent with the fact that PBP1b retains $\sim 75\%$ residual activity in assays employing a thioester substrate analogue in the presence of 1 mM S6 (Supplementary Table S1). These results

demonstrated the potential of aromatic boronic acids for binding to a clinically relevant PBP but suggested that the aryl boronates may not be optimal. We therefore switched our focus to alkyl-substituted acetamido boronic acids, some of which have been

Table 1. Inhibitory Activity of Boronate Ligands against PBP1b and Location of Their Respective Side Chains within the Active Site Cleft^a

 A1 - A5			 E6		 E7 - E10				
Compound	R	Pocket	Res. act. (%)	IC ₅₀ (μM)	Compound	R	Pocket	Res. act. (%)	IC ₅₀ (μM)
A1		2	67 ± 3 (1mM)	nd	A3		1	24 ± 1 (100μM)	26 ± 3
A2		1	20 ± 1 (100μM)	27 ± 1	A4		1	14 ± 4 (100μM)	16 ± 1
E6		1	39 ± 4 (1mM)	nd	A5		1	7 ± 3 (100μM)	6.9 ± 0.1
E7		2	29 ± 4 (100μM)	27 ± 2	E9		2	54 ± 1 (100μM)	nd
E8		2	81 ± 7 (100μM)	nd	E10		2	8 ± 6 (100μM)	20 ± 2

^aThe number in parentheses reflects the concentration of inhibitor employed in the thioester-based hydrolysis assay.

shown to be good inhibitors of the R39 transpeptidase,²² and tested them against PBP1b using a thioester-substrate-based hydrolysis assay. A number of these compounds, in particular glycine and alanine derivatives, were effective PBP1b inhibitors, with IC₅₀ values ranging from 6.9 to 27 μM (Table 1). Molecules carrying C-α derivatives larger than a methyl group were found to be either inactive or only poorly active (Supplementary Table S2). Notably, the nature of groups at the *ortho* position of the benzoyl side chain has a substantial positive effect on potency (Table 1). The 2,6-dimethoxy derivative A1, which is a good R39 inhibitor (IC₅₀ = 1.3 μM), is a poor inhibitor of PBP1b, displaying 67% residual activity even at a ligand concentration of 1 mM; similar results were observed with the (*R*)- and (*S*)-methyl-substituted analogues (Supplementary Table S2). However, the 2,6-difluoro analogue (A5) was active against PBP1b (IC₅₀ = 6.9 μM; Table 1). In addition to side chain structure, potency depends on the stereochemistry at the C-α center, with (*S*)-methyl-substituted analogues being superior inhibitors than their (*R*)-methyl-substituted enantiomers (i.e., E7 and E9 inhibit PBP1b better than E6 and E11, Table 1 and Supplementary Table S3). The difference in activity between the two enantiomers is dependent on the side chain structure. Introduction of a hydrophobic group at the *ortho* position of the aryl side chain increases potency, with several of the compounds having IC₅₀ values < 10 μM (i.e., E14 and E17, Supplementary Table S3), and the effects of 2,6-disubstitution with fluoro and hydrophobic groups are additive (compare A4 and A5, as well as E10 and E16, Table 1 and Supplementary Table S3).

Molecular Basis for Inhibitor Specificity. We then investigated the structural basis of the structure–activity relationships for boronic acid PBP inhibition by solving multiple high-resolution structures of PBP1b in complex with alkyl boronate ligands (Supplementary Tables S4–S6). In addition to the common formation of a covalent bond between Ser460 and the boron atom, several interactions within the active site are common to all of the structures (Figure 2). One of the boronic acid oxygen atoms is within hydrogen bonding distance of the O γ group of Ser516 (a catalytic residue located within the Ser-X-Asn motif) and, in all structures, also interacts with a Na⁺ ion, close to β 3. The second oxygen atom on the boronate points toward the oxyanion hole, which is formed by the backbone amides of Ser460 and Thr654. One of the oxygens of the boronate ester occupies a position close to that of the ester carbonyl of β -lactam-derived acyl–enzyme complexes⁸ (Supplementary Figure S1). The manner in which the boronic acids bind to the PBP active site is broadly similar to the manner in which boronic acid inhibitors bind to β -lactamases, at least as observed by crystallography. Ke *et al.*³⁰ have observed that the same boronic acid inhibitor adopts different conformations in the active sites of the TEM-1 and SHV-1 β -lactamases. Its positioning is proposed to better mimic the acylation or deacylation transition states when bound to TEM-1 (Supplementary Figure S2a) or SHV-1 (Supplementary Figure S2b), respectively. Notably, in our PBP-boronate structures, the position of the boronate ester is closer to the proposed acylation transition state mimic, as observed in the TEM-1 boronic inhibitor structure (Supplementary Figure S2a).

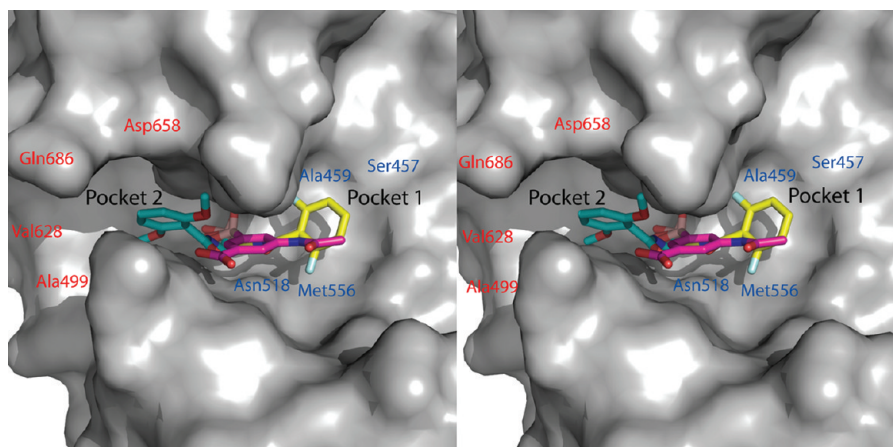


Figure 3. Overlay of the structures for complexes derived for three prototypic boronic acid ligands used in this study within the PBP1b active site. S6 is shown in pink, A5 in yellow, and A1 in cyan. Only molecules binding to Pocket 2 display antibacterial activity (stereo view).

The 10 co-crystal structures can be classified into two different “families”, depending on the pocket occupied by the ligand side chain within the active site. Five of the inhibitors (A2, A3, A4, and A5, all glycine analogues; and E6, a (*R*)-methyl-substituted analogue) possess aryl groups that occupy Pocket 1 (Figures 2b and 3 and Supplementary Figure S3). Pocket 1 is flat and formed mostly by the loops connecting $\alpha 6$, $\alpha 7$, and $\alpha 8$, as well as the loop leading to $\alpha 2$. This region is located toward the “back” of the active site, and thus the side chains are distant from the $\beta 3/\beta 4$ region of the site (the most malleable region of the catalytic cleft in several PBP^s^{27,29,31,32}), which is likely involved in substrate binding.

The PBP1b-A1 structure (Figure 2c) is taken as an example of ligands whose side chains fill Pocket 2 (Figure 3), such as E7, E8, E9, and E10 (Figure S2; the latter shown in detail in Figure 4). The C-6/C-7 amide side chain of cephalosporins and penicillins, including methicillin, which has a side chain closely related that of A1, also fills Pocket 2, though there are variations in the positioning of the aryl groups.⁸ In these structures, the aromatic rings are located proximally to the flexible $\beta 3/\beta 4$ loop region. Notably, the CH₃ group at the C- α position of most ligands in this category points into a groove formed by the Asn518 and Met556 side chains, which could explain why compounds with the *S*-stereochemistry analogues that carry a C- α group larger than a methyl moiety tend to display poor activity. Nevertheless, it is notable that analogues that occupy Pocket 2 display good inhibitory activity against PBP1b, with E10 displaying an IC₅₀ value of 20 μ M (with 8% and 0% residual activity at 100 μ M and 1 mM concentrations, respectively; Table 1). The structures of PBP1b in complex with molecules that occupy Pocket 2 also reveal that ligand binding causes a minor reorientation of Tyr498, potentially enabling π - π stacking interactions with the aromatic groups of the inhibitors. Interestingly, since (*R*)-methyl-substituted ligands occupy Pocket 1 and those with (*S*)-methyl substitutions occupy Pocket 2, C- α chirality may direct the side chain to a specific pocket. Overall, these results reveal the potential of boronic acids as effective PBP inhibitors and demonstrate the importance of a structure-based strategy for the analysis of inhibitor binding.

Bactericidal Activity and Specificity of *N*-Alkyl Boronates.

We then investigated the antibacterial spectrum of activity of the most potent alkyl boronic acid inhibitors by testing them against several Gram-positive and Gram-negative bacterial species, many

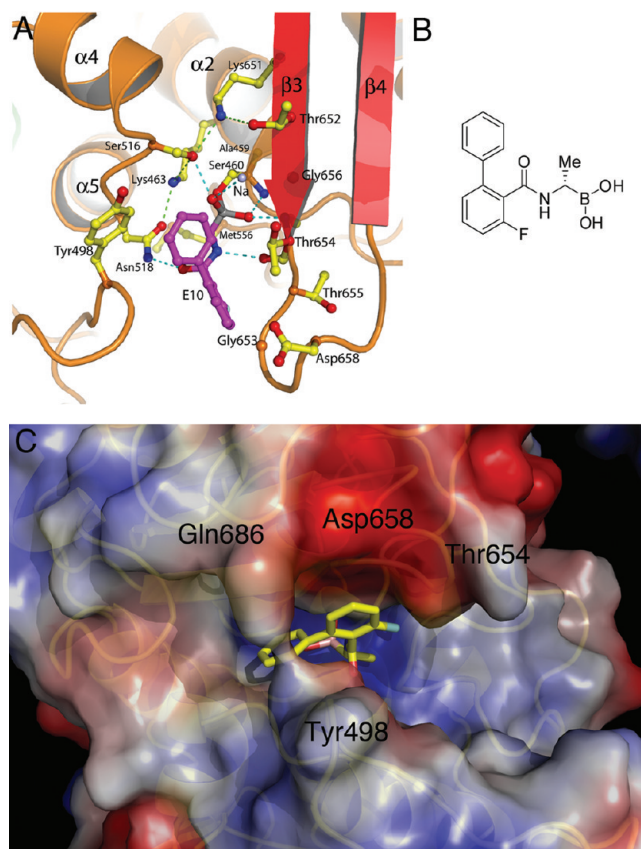


Figure 4. Constellation of interactions formed by PBP1b and molecule E10. (A) Interactions shown are those identified with the Ligplot program, used to generate Figure 2. (B) Chemical structure of molecule E10. (C) Electrostatic surface representation of PBP1b complexed to E10 from a different orientation from that in panel A, where both rings can be clearly seen. The elongated PBP substrate binding site is also clearly visible. The boron atom is represented in pink, and fluorine in cyan.

of which are human pathogens. Of the 19 species tested, 11 showed cellular growth inhibition in the presence of three molecules (E9, E10, and E16), including a methicillin-resistant strain of *Staphylococcus aureus* (MRSA) that expresses a low

Table 2. Minimum Inhibitory Concentration (MIC, $\mu\text{g/mL}$) Values for Different Boronic Acid Analogues against Gram-Positive Organisms

bacterial strain	E9	E16	E10
<i>Bacillus subtilis</i> ATCC 6633	256	32	16
<i>Listeria monocytogenes</i> ATCC 14780	256	64	32
<i>Listeria innocua</i> ATCC 33090	256	64	32
<i>Enterococcus hirae</i> ATCC 8790	128	32	32
<i>Enterococcus faecalis</i> ATCC 19433	>256	32	128
<i>Enterococcus faecalis</i> ATCC 29212	>256	32	128
<i>Enterococcus faecium</i> ATCC 19434	256	128	128
<i>Staphylococcus epidermidis</i> ATCC 12228	256	64	16
<i>Staphylococcus aureus</i> ATCC 25923	256	64	32
<i>Staphylococcus aureus</i> PL 1 (inducible MRSA)	256	128	32
<i>Staphylococcus aureus</i> ATCC 43300 (MRSA)	32	128	32

β -lactam affinity PBP (PBP2a; MIC_{ampicillin} = 256 $\mu\text{g/mL}$) (Table 2). It is of note that all of the species that were inhibited by boronic acids are Gram-positive organisms, suggesting that the outer membrane, efflux mechanisms, or differential usage of peptidic substrates by Gram-negative microorganisms could play a role in affecting efficacy of the tested compounds in these species. Notably, the structures of PBP1b in complex with E9 and E10 (Supplementary Figure S4 and 3) reveal that their side chains both fill Pocket 2. It is of interest that none of the molecules whose side chains fill Pocket 1 displayed any antibacterial activity (not shown). These observations suggest that there may be a correlation between inhibitor side chain orientation within the PBP active site and antibacterial efficacy.

On the basis of these results, we selected compound E10 for detailed analysis and tested its effect on MRSA. MRSA liquid cultures were grown either in the absence or in the presence of increasing amounts of E10 for up to 24 h (Figure 5a), and the number of colony-forming units (CFU mL⁻¹) was determined at different time points. At levels corresponding to 0.5 times the MIC and at the MIC, E10 induced a bacteriostatic effect, blocking growth, while at higher concentrations the CFU mL⁻¹ dropped rapidly (leading to over 2 log reductions in CFU mL⁻¹ after 24 h, compared to the untreated control), revealing that E10 is bactericidal. These results suggest that one or more essential PBPs are inhibited.

MRSA displays a wide spectrum of resistance to all β -lactam antibiotics. *S. aureus* produces four natural PBPs, two of which (PBP1 and PBP2) are essential for growth;^{33,34} an additional enzyme, PBP2a, is expressed by strains resistant to β -lactam antibiotics (such as the one employed in this study, ATCC 43300). To test whether PBPs are being directly inhibited by E10, membrane-enriched fractions were purified from MRSA cells grown to late exponential phase and PBPs were probed with fluorescent ampicillin either in the presence or absence of E10. The membrane fraction was subsequently analyzed by SDS-PAGE and fluorescence imaging, and the percentage of inhibition was quantified (Figure 5b). The untreated, control lane shows that all staphylococcal PBPs are identified: PBP1, PBP2, PBP2a (which comigrates with PBP2 on SDS-PAGE), PBP3, and PBP4. E10-treated membranes, however, display a clear inhibition of PBP1 even at half the MIC value (87%). PBP2 and PBP2a cannot be separated on SDS-PAGE,³³ but even at the lowest concentration employed in the assay, the “double” PBP2/PBP2a band is also clearly less intense (15% inhibition at 0.5 times the MIC),

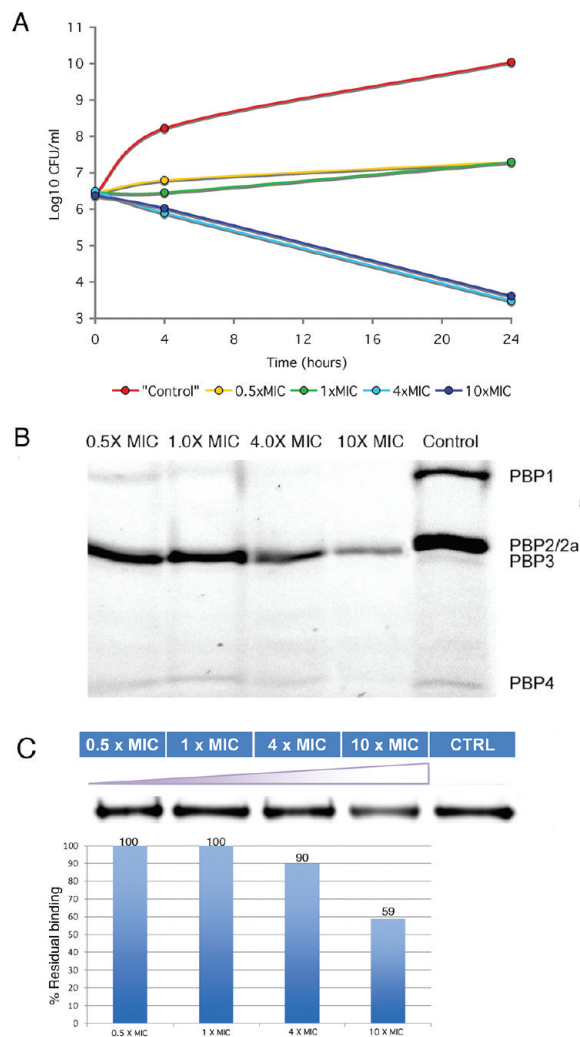


Figure 5. Inhibitor E10 shows anti-MRSA activity and targets specific PBPs. (A) Killing curves of MRSA as a function of time in absence (control) or presence of 0.5, 1, 4, and 10 times the MIC of E10. Time points were taken at 0, 4, and 24 h for three independent experiments. (B) MRSA membrane preparations preincubated with E10 prior to addition of fluorescent ampicillin reveals that PBP1, an essential enzyme, is the first one to be targeted. At 4.0 times the MIC (point at which E10 becomes bactericidal), PBP1 is inhibited by 100%, PBP2/2a by 43%, PBP3 by 100%, and PBP4 by 40%, as measured by fluorescence scanning. (C) Inhibition of purified, low affinity PBP2a by the same quantities of E10 used in panels A and B, employing a fluorescent ampicillin-based assay. Clear inhibition occurs at 4 and 10 times the MIC values, as in the previous experiments.

suggesting that these proteins are targeted. PBP3, which is seen as a light band under the PBP2/PBP2a band in the control lane, is absent from all of the lanes in which E10 was added, suggesting 100% inhibition. At 4.0 times the MIC, the point at which E10 becomes bactericidal, all PBPs are affected, as shown by their decreased ability to stably bind fluorescently labeled β -lactam in the presence of the inhibitor. These results are confirmed by experiments performed with purified PBP2a, which indicate clear detection of inhibition at 4 and 10 times the MIC (Figure 5c).

PBP1 is a class B PBP that is essential for staphylococcal growth; PBP1 deletion mutants are unable to divide and continuously enlarge in size, and display cell walls with decreased levels of cross-linking.^{33,35} In addition, inhibition of the TP

activity of PBP1 blocks the autolytic system of *S. aureus*, which affects cell separation during the division process, generating cell doublets and tetrads.³³ Notably, it has also been shown that the PBP3-encoded TP activity, which also plays a role in autolysis, can be substituted for by PBP1 in PBP3 deletion mutants,³⁶ highlighting the importance of the interplay between these two enzymes in staphylococcal growth and division. The fact that PBP1 is particularly sensitive to E10 suggests that this inhibitor may directly target the staphylococcal autolysis system. The collective results support an inhibitory action of alkyl boronates on multiple membrane-localized PBPs through the formation of reversibly-formed tetrahedral complexes involving occupation of Pocket 2 within PBP active sites, leading to inhibition of peptidoglycan cross-linking, affecting autolysis, and resulting in a bactericidal effect. A boronic acid-based proteasome inhibitor is currently in clinical use,³⁷ suggesting that the alkyl boronic acid analogues described here may represent useful lead molecules for the development of clinically tractable therapeutics against β -lactam-resistant pathogens.

METHODS

Inhibition Assays. PBP1b (0.2 μ M) was incubated with boronic acids in 10 mM sodium phosphate buffer (pH 7.0) in the presence of 100 mM D-alanine and 0.01 mg mL⁻¹ BSA for 60 min at 25 °C. Residual activities were determined from initial rates of the hydrolysis of a thioester 2-(2-benzamidopropanoylthio) acetic acid (synthesis will be described elsewhere), used as reporter substrate at a concentration of 5 mM. After preincubation, the initial rate of thioester hydrolysis and of spontaneous hydrolysis ($\epsilon[\Delta\epsilon]_{412\text{ nm}} = 13,600\text{ M}^{-1}\text{ cm}^{-1}$) were measured in the presence of 1 mM DTNB using a microtiter 96-well plate and a Power Wave microtiter plate reader (Bio-Tek Instruments; total volume of tests was 150 μ L). All experiments were done in duplicate. Activity of PBP1b in absence of inhibitors (100% RA) was measured by performing six replicates on each plate. In order to minimize the detection of false positives (promiscuous inhibitors), which show no inhibition in the presence of Triton-X-100,^{38,39} all assays were done in the presence of 0.01% Triton-X-100. If inhibition was detected, residual activity (RA) was measured over a range of concentrations from which IC₅₀ values were determined by performing a nonlinear regression analysis using Sigma Plot (Systat software) and fitting the data to the equation $y = y_0 + (a \times b)/(b + x)$ as in ref 13.

PBP1b Mutagenesis, Purification, and Crystallization. Mutation Asn656Gly was introduced in the *pbp1b* gene by employing the QuikChange II Site-Directed Mutagenesis kit (Stratagene). The reaction was performed directly on the expression vector pGEX4T expressing the PBP1b triple mutant Arg336Gln/Arg686Gln/Arg687Gln, described previously in refs 27 and 40. The presence of the desired mutation was confirmed by DNA sequencing, and the quadruple mutant is referred to simply as PBP1b in the text.

PBP1b was purified as described for native PBP1b,⁴⁰ with minor modifications. Notably, trypsinization of GST-PBP1b was performed while the protein was still associated to the glutathione-Sepharose column. Eluted protein was subsequently loaded and eluted from a Superdex 200 HR10/30 Sepharose column (GE Healthcare) in 50 mM HEPES pH 7.0, 0.1 M NaCl, 1 mM EDTA. Pooled peak fractions were concentrated to 8.5 mg mL⁻¹ and crystallized in 50 mM HEPES pH 7.2, 3 M NaCl, 0.6–0.9 M ammonium sulfate. Crystal soaks were performed by slowly adding ligands prepared in either DMSO or H₂O (in concentrations in the range of 15 mM) directly to the crystallization drop (in a final volume of 2 μ L).

Data Collection and Structure Solution. All data were collected at the European Synchrotron Radiation Facility (Grenoble) on

beamlines ID14-EH1, ID23-1, ID23-2 and ID29 and were processed using the program XDS.⁴¹ Structures were solved by molecular replacement using the program PHASER⁴² and employing the coordinates of PBP1b (PDB code 2bg4) lacking residues 460, 516–518, and 650–661 as a model. The models were then rebuilt *de novo* with ARP/wARP (7.1.1)⁴³ and Lafire 3.02⁴⁴ to remove bias. Cycles of restrained refinement employing NCS and TLS refinement were performed with REFMAC 5.5⁴⁵ as implemented in the CCP4 6.1.13 program suite. All solved structures displayed between 99.5% and 100% of the non-glycine residues in the most favored and allowed regions of the Ramachandran plot.⁴⁶ Ligand–protein interactions were analyzed with LigPlot 1.1.⁴⁷ Due to the high concentration of NaCl employed in crystallization as well as optimal H-bonding parameters, a Na⁺ ion was modeled into a sphere of high electron density within the active site. Stereochemical verification was performed by PROCHECK⁴⁶ and secondary structure assignment by DSSP.⁴⁸ Data collection and refinement statistics are included in Supplementary Tables S3–S5. Figures were generated with PyMol (<http://www.pymol.org>).

MIC Determination. Tests were made using microtitration plates, in 200 μ L (final volume) of Mueller-Hinton Broth (MHB), following EUCAST (European Committee on Antimicrobial Susceptibility testing)/CLSI (Clinical and Laboratory Standard Institute) recommended procedures. Inhibitors were solubilized in 100% DMF and then diluted in MHB, just before utilization. Inoculums were prepared for each strain, resuspending isolated colonies from plates that had been cultured for 18 h. Equivalents of 0.5 MacFarland turbidity standard (approximately 1×10^8 CFU mL⁻¹) were prepared in saline solution (NaCl 0.085%) and then diluted 200-fold in MBH (initial population). MIC values were determined as the lowest dilution of product showing no visual turbidity. Strains that were tested but were not susceptible to the ligands described in this work include *E. coli* (ATCC 8739), *Proteus mirabilis* (ATCC 29936), *Klebsiella pneumoniae* (ATCC 13883), *Citrobacter freundii* (ATCC 8090), *Pseudomonas aeruginosa* (ATCC 27853), *Micrococcus luteus* (ATCC 9341), and *Streptococcus pneumoniae* (ATCC 49619/ATCC 34400).

Time-Kill Assay. *Staphylococcus aureus* ATCC 43300 (MRSA) was purchased from BCCM/LMG Laboratorium voor Microbiologie, Universiteit Gent (UGent), Belgium. Cation-adjusted MHB, supplemented with 20% agar–agar for colony counts, was employed for the test. Inhibitors were solubilized in 100% DMF and then diluted 50-fold in MHB, just before utilization. Bacterial inoculums were prepared by suspending two or three colonies, isolated from an overnight cultured plate of Mueller-Hinton agar, in 0.9% NaCl to obtain the equivalent turbidity of the 0.5 McFarland standard tube. The suspension was subsequently diluted 100-fold diluted in MHB and aliquotted, and ligand E10 was added to yield 0.5, 1, 4, or 10 times the respective MIC value. The suspensions were mixed, and samples were taken at 0, 4, and 24 h. The samples were serially diluted, plated on Mueller-Hinton agar, and incubated overnight. The mean number of survivors was determined.

Membrane Extraction and PBP Profiles. Cytoplasmic membrane fractions were prepared from late exponential phase staphylococcal cultures. Cells were recovered by centrifugation (13,000g, 10 min), washed once in 10 mM Tris-HCl pH 7.0, and resuspended in the same buffer. The cells were disrupted through 5 passages through a French-Press and the cell wall debris was removed by centrifugation (13,000g, 10 min). To isolate the cytoplasmic membrane fraction, the supernatant was subjected to ultracentrifugation (Beckman ultracentrifuge; 130,000g for 1 h at 4 °C), and the pellet was suspended in 10 mM Tris-HCl pH 7.0. The protein content of the samples was quantified using a BSA Protein Quantification kit (Pierce) as per manufacturer's instructions. PBPs in membrane preparations were selectively labeled by preincubation of the samples (200 μ g proteins) with concentrations of E10 corresponding to 0.5, 1, 4, and 10 times the MIC for 4 h at 30 °C and then counterlabeled with 25 μ M of fluorescent ampicillin. The proteins in the sample were separated by SDS-PAGE, and the PBPs were detected with a Bio-Rad

Molecular Imager FX. Quantification of inhibition was performed by employing Quantity One software (BioRad, Hercules, CA, USA) after subtraction of background fluorescence. Relative PBP inhibition was calculated as

$$\%inhibition = \left[\frac{1 - \text{intensity of PBP band pre-incubated with E10}}{\text{intensity of PBP band without inhibitor}} \right] \times 100$$

Experiments were carried out in triplicate.

Inhibition Test for Low Affinity PBP2a. PBP2a from *S. aureus* ATCC 43300 was overproduced and purified as described in ref 49. PBP2a (2.5 μM) was first made to react with 0.5, 1, 4 and 10 times the MIC value of inhibitor E10 in 100 mM phosphate buffer pH 7.0 (with 0.01% Triton X-100) for 30 min at 37 °C. The same amount of PBP2a without inhibitor was incubated under identical conditions as a control (100% residual β -lactam binding activity, RA). Since the thioester employed for PBP1b experiments is not a substrate for PBP2a, we used a method involving incubation of PBP2a with fluorescein-labeled ampicillin (25 μM) and subsequent analysis by SDS-PAGE in order to detect residual binding.⁵⁰ Samples were further incubated for 30 min at 37 °C in a total volume of 20 μL . Denaturation buffer was added and samples were heated to 100 °C for 1 min. Samples were subsequently loaded on a 10% SDS-PAGE, and detection and quantification of RA were made with Molecular Image FX equipment and Quantity One software (BioRad, Hercules, CA, USA). Results are the mean from three independent experiments.

Compound Synthesis. Details of synthetic methods are given in Supporting Information.

■ ASSOCIATED CONTENT

S Supporting Information. Figures of the structures of PBP1b complexed to eight boronates, crystallography tables, tables describing kinetic measurements for boronates that were not tested for complexation with PBP1b by X-ray crystallography, and chemical syntheses. This material is available free of charge via the Internet at <http://pubs.acs.org>.

■ AUTHOR INFORMATION

Corresponding Author

*E-mail: christopher.schofield@chem.ox.ac.uk; andrea.dessen@ibs.fr.

Author Contributions

[†]These authors contributed equally to this work.

■ ACKNOWLEDGMENT

The authors wish to thank the European Synchrotron Radiation Facility (ESRF) staff (Partnership for Structural Biology) for help with data collection. This work was supported by grants from the European Commission (LSHM-CT-2004-512138), the Belgian Program on Interuniversity Poles of Attraction, initiated by the Belgian State (grant P6/19; to B.J.) and the Fondation pour la Recherche Médicale (FRM DEQ20090515390; to A.D.). The coordinates of the PBP1b complex structures have been deposited in the Protein Data Bank.

■ REFERENCES

(1) Fischbach, M. A., and Walsh, C. T. (2009) Antibiotics for emerging pathogens. *Science* 325, 1089–1093.

(2) Eliopoulos, G. M. (2009) Microbiology of drugs for treating multiply drug-resistant Gram-positive bacteria. *J. Infect.* 59, S17–S24.

(3) Hölftje, J. V. (1998) Growth of the stress-bearing and shape-maintaining murein sacculus of *Escherichia coli*. *Microbiol. Mol. Biol. Rev.* 62, 181–203.

(4) Sauvage, E., Kerff, F., Terrak, M., Ayala, J. A., and Charlier, P. (2008) The penicillin-binding proteins: structure and role in peptidoglycan biosynthesis. *FEMS Microbiol. Rev.* 32, 234–258.

(5) Mattei, P.-J., Neves, D., and Dessen, A. (2010) Bridging cell wall biosynthesis and bacterial morphogenesis. *Curr. Opin. Struct. Biol.* 20, 749–766.

(6) Vollmer, W., and Bertsche, U. (2008) Murein (peptidoglycan) structure, architecture and biosynthesis in *Escherichia coli*. *Biochim. Biophys. Acta* 1778, 1714–1734.

(7) Morlot, C., Pernot, L., Le Gouellec, A., Di Guilmi, A. M., Vernet, T., Dideberg, O., and Dessen, A. (2005) Crystal structure of a peptidoglycan synthesis regulatory factor (PBP3) from *Streptococcus pneumoniae*. *J. Biol. Chem.* 280, 15984–15991.

(8) Lim, D., and Strynadka, N. C. (2002) Structural basis for the β -lactam resistance of PBP2a from methicillin-resistant *Staphylococcus aureus*. *Nat. Struct. Biol.* 9, 870–876.

(9) Contreras-Martel, C., Dahout-Gonzalez, C., Dos Santos Martins, A., Kotnik, M., and Dessen, A. (2009) PBP active site flexibility as the key mechanism for β -lactam resistance in pneumococci. *J. Mol. Biol.* 387, 899–909.

(10) Contreras-Martel, C., Job, V., Di Guilmi, A. M., Vernet, T., Dideberg, O., and Dessen, A. (2006) Crystal structure of Penicillin-Binding Protein 1a (PBP1a) reveals a mutational hotspot implicated in β -lactam resistance in *Streptococcus pneumoniae*. *J. Mol. Biol.* 355, 684–696.

(11) Sauvage, E., Kerff, F., Fonze, E., Herman, R., Schoot, B., Marquette, J. P., Taburet, Y., Prevost, D., Dumas, J., Leonard, G., Stefanic, P., Coyette, J., and Charlier, P. (2002) The 2.4 Å crystal structure of the penicillin-resistant penicillin-binding protein PBP5fm from *Enterococcus faecium* in complex with benzylpenicillin. *Cell. Mol. Life Sci.* 59, 1223–1232.

(12) Rice, L. B. (2009) The clinical consequences of antimicrobial resistance. *Curr. Opin. Microbiol.* 12, 476–481.

(13) Macheboeuf, P., Fischer, D. S., Brown, T., Jr., Zervosen, A., Luxen, A., Joris, B., Dessen, A., and Schofield, C. J. (2007) Structural and mechanistic basis of penicillin-binding protein inhibition by lactvicins. *Nat. Chem. Biol.* 3, 565–569.

(14) Nozaki, Y., Katayama, N., Ono, H., Tsubotani, S., Harada, S., Okazaki, H., and Nakao, Y. (1987) Binding of a non- β -lactam antibiotic to penicillin-binding proteins. *Nature* 325, 179–180.

(15) Brown, T. J., Charlier, P., Herman, R., Schofield, C. J., and Sauvage, E. (2010) Structural basis for the interaction of lactvicins with serine beta-lactamases. *J. Med. Chem.* 53, 5890–5894.

(16) Crompton, I. E., Cuthbert, B. K., Lowe, G., and Waley, S. G. (1988) The inhibition of serine β -lactamases by specific boronic acids. *Biochem. J.* 251, 453–459.

(17) Nicola, G., Peddi, S., Stefanova, M., Nicholas, R. A., Gutheil, W. G., and Davies, C. (2005) Crystal structure of *Escherichia coli* penicillin-binding protein 5 bound to a tripeptide boronic acid inhibitor: a role for Ser-110 in deacylation. *Biochemistry* 44, 8207–8217.

(18) Pechenov, A., Stefanova, M. E., Nicholas, R. A., Peddi, S., and Gutheil, W. G. (2003) Potential transition state analogue inhibitors for the penicillin-binding proteins. *Biochemistry* 42, 579–588.

(19) Ness, S., Martin, R., Kindler, A. M., Paetzel, M., Gold, M., Jensen, S. E., Jones, J. B., and Strynadka, N. C. (2000) Structure-based design guides the improved efficacy of deacylation transition state analogue inhibitors of TEM-1 β -lactamase. *Biochemistry* 39, 5312–5321.

(20) Powers, R. A., Blazquez, J., Weston, G. S., Morosini, M.-I., Baquero, F., and Shoichet, B. K. (2007) The complexed structure and antimicrobial activity of a non- β -lactam inhibitor of AmpC β -lactamase. *Protein Sci.* 8, 2330–2337.

(21) Inglis, S. R., Zervosen, A., Woon, E. C. Y., Gerards, T., Teller, N., Fischer, D. S., Luxen, A., and Schofield, C. (2009) Synthesis and

evaluation of 3-(dihydroxyboryl) benzoic acids as D,D-carboxypeptidase R39 inhibitors. *J. Med. Chem.* 52, 6097–6106.

(22) Woon, E. C. Y., Zervosen, A., Sauvage, E., Simmons, K. J., Zivec, M., Inglis, S. R., Fishwick, C. W. G., Gobec, S., Charlier, P., Luxen, A., and Schofield, C. J. (2011) Structure guided development of potent reversibly binding Penicillin-Binding Protein inhibitors. *ACS Med. Chem. Lett.* 2, 219–223.

(23) Morandi, F., Caselli, E., Morandi, S., Focia, P. J., Blazquez, J., Shoichet, B. K., and Prati, F. (2003) Nanomolar inhibitors of AmpC β -lactamase. *J. Am. Chem. Soc.* 125, 685–695.

(24) Weston, G. S., Blazquez, J., Baquero, F., and Shoichet, B. K. (1998) Structure-based enhancement of boronic acid-based inhibitors of AmpC β -lactamase. *J. Med. Chem.* 41, 4577–4586.

(25) Caselli, E., Powers, R. A., Blaszczak, L. C., Wu, C. Y. E., Prati, F., and Shoichet, B. K. (2001) Energetic, structural, and antimicrobial analyses of β -lactam side chain recognition by β -lactamases. *Chem. Biol.* 8, 17–31.

(26) Drawz, S. M., Babic, M., Bethel, C. R., Taracila, M., Distler, A. M., Ori, C., Caselli, E., Prati, F., and Bonomo, R. A. (2010) Inhibition of the class C β -lactamase from *Acinetobacter* spp.: insights into effective inhibitor design. *Biochemistry* 49, 329–340.

(27) Macheboeuf, P., Di Guilmi, A. M., Job, V., Vernet, T., Dideberg, O., and Dessen, A. (2005) Active site restructuring regulates ligand recognition in class A penicillin-binding proteins. *Proc. Natl. Acad. Sci. U.S.A.* 102, 577–582.

(28) Dessen, A., Mouz, N., Gordon, E., Hopkins, J., and Dideberg, O. (2001) Crystal structure of PBP2x from a highly penicillin-resistant *Streptococcus pneumoniae* clinical isolate. *J. Biol. Chem.* 276, 45106–45112.

(29) Macheboeuf, P., Lemaire, D., Thaller, N., Dos Santos Martins, A., Luxen, A., Dideberg, O., Jamin, M., and Dessen, A. (2007) Trapping of an acyl-enzyme intermediate in a penicillin-binding protein (PBP) catalyzed reaction. *J. Mol. Biol.* 376, 405–413.

(30) Ke, W., Sampson, J. M., Ori, C., Prati, F., Drawz, S. M., Bethel, C. R., Bonomo, R. A., and van den Akker, F. (2011) Novel insights into the mode of inhibition of class A SHV-1 β -lactamases revealed by boronic acid transition state inhibitors. *Antimicrob. Agents Chemother.* 55, 174–183.

(31) Fedarovich, A., Nicholas, R. A., and Davies, C. (2010) Unusual conformation of the SXN motif in the crystal structure of Penicillin-Binding Protein A from *Mycobacterium tuberculosis*. *J. Mol. Biol.* 398, 54–65.

(32) Chen, Y., Zhang, W., Shi, Q., Hesek, D., Lee, M., Mobashery, S., and Shoichet, B. K. (2009) Crystal structures of penicillin-binding protein 6 from *Escherichia coli*. *J. Am. Chem. Soc.* 131, 14345–14354.

(33) Pereira, S. F. F., Henriques, A. O., Pinho, M. G., de Lencastre, H., and Tomasz, A. (2009) Evidence for a dual role of PBP1 in the cell division and cell separation of *Staphylococcus aureus*. *Mol. Microbiol.* 72, 895–904.

(34) Pinho, M. G., Filipe, S. R., de Lencastre, H., and Tomasz, A. (2001) Complementation of the essential peptidoglycan transpeptidase function of Penicillin-Binding Protein 2 (PBP2) by the drug resistance protein PBP2a in *Staphylococcus aureus*. *J. Bacteriol.* 183, 6525–6531.

(35) Pereira, S. F. F., Henriques, A. O., Pinho, M. G., de Lencastre, H., and Tomasz, A. (2007) role of PBP1 in cell division of *Staphylococcus aureus*. *J. Bacteriol.* 189, 3525–3531.

(36) Pinho, M. G., de Lencastre, H., and Tomasz, A. (2000) Cloning, characterization, and inactivation of the gene *pbpC*, encoding penicillin-binding protein 3 of *Staphylococcus aureus*. *J. Bacteriol.* 182, 1074–1079.

(37) Kropff, M., Bisping, G., Schuck, E., Liebisch, P., Lang, N., Hentrich, M., Dechow, T., Kroger, N., Salwender, H., Metzner, B., Sezer, O., Engelhardt, M., Wolf, H.-H., Einsele, H., Volpert, S., Heinecke, A., Berdel, W. E., Kienast, J., and Myelom, D. S. M. (2007) Bortezomib in combination with intermediate-dose dexamethasone and continuous low-dose oral cyclophosphamide for relapsed multiple myeloma. *Br. J. Haematol.* 138, 330–337.

(38) Feng, B. Y., and Shoichet, B. K. (2006) A detergent-based assay for the detection of promiscuous inhibitors. *Nat. Protoc.* 1, 550–553.

(39) Shoichet, B. K. (2006) Screening in a spirit haunted world. *Drug Discovery Today* 11, 607–615.

(40) Di Guilmi, A. M., Dessen, A., Dideberg, O., and Vernet, T. (2003) Functional characterization of Penicillin-Binding Protein 1b from *Streptococcus pneumoniae*. *J. Bacteriol.* 185, 1650–1658.

(41) Kabsch, W. (1993) Automatic processing of rotation diffraction data from crystals of initially unknown symmetry and cell constants. *J. Appl. Crystallogr.* 26, 795–800.

(42) Storoni, L., McCoy, A., and Read, R. (2004) Likelihood-enhanced fast rotation functions. *Acta Crystallogr., Sect. D* 57, 1373–1382.

(43) Cohen, S. X., Ben Jelloul, M., Long, F., Vagin, A., Knipscheer, P., Lebbink, J., Sixma, T. K., Lamzin, V. S., Murshudov, G. N., and Perrakis, A. (2008) ARP/wARP and molecular replacement: the next generation. *Acta Crystallogr., Sect. D* 64, 49–60.

(44) Yao, M., Zhou, Y., and Tanaka, I. (2006) LAFIRE: software for automating the refinement process of protein structure analysis. *Acta Crystallogr., Sect. D* 62, 189–196.

(45) Murshudov, G., Vagin, A., and Dodson, E. (1997) Refinement of macromolecular structures by the maximum-likelihood method. *Acta Crystallogr., Sect. D* 53, 240–255.

(46) Laskowski, R. A., MacArthur, M. W., Moss, D. S., and Thornton, J. M. (1993) PROCHECK: a program to check the stereo chemical quality of protein structures. *J. Appl. Crystallogr.* 26, 283–291.

(47) Wallace, A. C., Laskowski, R. A., and Thornton, J. M. (1995) LIGPLOT: A program to generate schematic diagrams of protein-ligand interactions. *Protein Eng.* 8, 127–134.

(48) Kabsch, W., and Sander, C. (1983) Dictionary of protein secondary structure: pattern recognition of hydrogen-bonded and geometrical features. *Biopolymers* 22, 2577–2637.

(49) Lemaire, S., Glupczynski, Y., Duval, V., Joris, B., Tulkens, P. M., and Van Bambeke, F. (2009) Activities of ceftobiprole and other cephalosporins against extracellular and intracellular (THP-1 macrophages and keratinocytes) forms of methicillin-susceptible and methicillin-resistant *Staphylococcus aureus*. *Antimicrob. Agents Chemother.* 53, 2289–2297.

(50) Lakaye, B., Damblon, C., Jamin, M., Galleni, M., Lepage, S., Joris, B., Marchand-Brynaert, J., Frydrych, C., and Frère, J.-M. (1994) Synthesis, purification and kinetic properties of fluorescein-labelled penicillins. *Biochem. J.* 300, 141–145.